

# Acoustic temperature measurement in a rocket noise field

Jarom H. Giraud, Kent L. Gee,<sup>a)</sup> and John E. Ellsworth

*Department of Physics and Astronomy, Brigham Young University, Provo, Utah 84602*  
*jaromgiraud@gmail.com, kentgee@byu.edu, jee@physics.byu.edu*

**Abstract:** A 1  $\mu\text{m}$  diameter platinum wire resistance thermometer has been used to measure temperature fluctuations generated during a static GEM-60 rocket motor test. Exact and small-signal relationships between acoustic pressure and acoustic temperature are derived in order to compare the temperature probe output with that of a 3.18 mm diameter condenser microphone. After preliminary plane wave tests yielded good agreement between the transducers within the temperature probe's  $\sim 2$  kHz bandwidth, comparison between the temperature probe and microphone data during the motor firing show that the  $\pm \sim 3$  K acoustic temperature fluctuations are a significant contributor to the total temperature variations.

© 2010 Acoustical Society of America

**PACS numbers:** 43.20.Ye, 43.50.Nm [AN]

**Date Received:** February 12, 2010 **Date Accepted:** March 17, 2010

## 1. Introduction

Measurement of acoustic field variables has traditionally relied on one or more microphones for the sensing of acoustic pressure from which other quantities are calculated. Direct measurement of acoustic temperature is very uncommon, but may be accomplished through the use of thin wire resistance thermometers similar to those developed for high-frequency atmospheric temperature measurements in the 1960s and 1970s.<sup>1-4</sup> The thermometers use a constant current supplied to the wire, whose resistance varies with temperature in a known fashion. A change in temperature, and therefore resistance, is then related to a measurable voltage through Ohm's law. These probes differ from hot-wire anemometers and a commercially available particle velocity sensor<sup>5</sup> in that the current is kept small such that flow does not appreciably alter the wire's temperature.<sup>2</sup> This approach allows for the measurement of temperature variations not related to mean flow, i.e., acoustic temperature.

Some work related to acoustic temperature measurements has been reported before in closed systems. Huelsz and Ramos<sup>6</sup> measured temperature fluctuations in the boundary layer of a waveguide and then later<sup>7</sup> used the same techniques to experimentally examine thermoacoustic power production in a tube. A thin wire probe has also been used to determine temperature fluctuations caused by shocks in a tube, which was done with the intent of correcting the effect of temperature fluctuations on the performance of a hot-wire probe.<sup>8</sup>

Although acoustic temperature measurements in a high-amplitude plane wave tube are discussed, the primary purpose of this letter is to describe acoustic temperature measurements made during a large solid-fuel rocket motor firing, where nonacoustic temperature fluctuations are also present. A secondary purpose for these measurements was pedagogical because acoustic temperature measurements can be educational for advanced students of acoustics. Despite knowledge of the thermodynamic relationship between acoustic temperature and pressure, acoustic temperature fluctuations are not "experienced" the same as pressure waves because of the thermal inertia of our skin. (It is possible that for this reason Newton incorrectly hypothesized that sound propagation was isothermal, rather than adiabatic.) On the other hand, the pressure oscillations produced near intense sound sources can be both felt and heard.

---

<sup>a)</sup> Author to whom correspondence should be addressed.

## 2. Acoustic temperature as a function of pressure

To verify the temperature fluctuations registered by a thin wire probe are acoustic, it is useful to define the relationship between acoustic pressure and acoustic temperature in air to allow microphone data to serve as a benchmark. The total quantities of density,  $\rho$ , temperature in Kelvin,  $T_K$ , and pressure,  $P$ , can be defined as the sum of an ambient mean and an acoustic deviation (e.g.,  $\rho = \rho_0 + \Delta\rho$ ). The temperature variation,  $\Delta T_k$ , can be derived from the perfect gas adiabat  $P/P_0 = (\rho/\rho_0)^\gamma$ , where  $\gamma$  is the ratio of specific heats, by substituting  $\rho/\rho_0 = PT_{K0}/P_0T_K$ . The resulting equation can be solved for  $T_K$ , to yield

$$T_K = T_{K0} \left( 1 + \frac{\Delta P}{P_0} \right)^{(\gamma-1)/\gamma}. \quad (1)$$

Equation (1), although exact for adiabatic oscillations in a perfect gas, may be simplified to find a linear relationship between  $\Delta T_k$  and  $\Delta P$  by assuming  $\Delta P/P_0 \ll 1$ . A binomial expansion of Eq. (1) results in

$$\Delta T_K = \Delta P \left( \frac{\gamma-1}{\gamma} \right) \frac{T_{K0}}{P_0}. \quad (2)$$

Equation (2) agrees with the results in Refs. 9–11, whose authors arrive at Eq. (2) from different approaches. [For example, Eq. (2) can also be found if we start with the ideal gas equation of state for  $P$ ,  $T_K$ , and  $\rho$  and directly utilize the small-signal relationship  $\Delta P \approx c_0^2 \Delta\rho$ , where  $c_0$  is the speed of sound, when solving for  $\Delta T_k$ .] A comparison of the relative error between Eqs. (1) and (2) at 20 °C and 1 atm shows that it is only as the acoustic pressure approaches 80 kPa (192 dB re 20  $\mu$ Pa) and  $\Delta T_k$  approaches 50 K that the error reaches 1 dB. Note that a temperature wave with amplitude 1 K corresponds to an acoustic pressure amplitude of about 1220 Pa (156 dB re 20  $\mu$ Pa) and the standard “reference” temperature for a 0 dB, 1 pW/m<sup>2</sup> plane wave at 1 atm and 20 °C is approximately 17 nK.

## 3. Temperature fluctuations in a nonlinearly propagating plane wave

Initial laboratory experiments were performed using a high-amplitude plane wave tube to compare the output of a 3.8 mm GRAS 40DP pressure microphone to the Dantec Dynamics temperature probe used. The Dantec 55P31 probe is a single 0.4 mm long, 1  $\mu$ m diameter platinum wire spot welded to stainless steel prongs. The probe, powered by a constant current supply of about 0.8 mA, had a noise floor of about 170  $\mu$ K (80 dB re 17 nK). Including signal conditioning, its sensitivity was approximately 12.8 °C/volt, which was found by calibration relative to the 40DP microphone in the plane wave tube. The 5.1 cm inner diameter, 9 m long plane wave tube is constructed of schedule 40 PVC pipe with an anechoic termination and is driven by three directly coupled BMS 4591 compression drivers. Data acquisition was carried out using a National Instruments PXI-4462 card with a 204.8 kHz sampling frequency. The acoustic pressure measured by the 40DP microphone was converted to an acoustic temperature using Eq. (2) and compared to the measurement obtained by the temperature probe. A representative case with significant temperature oscillations approaching 1 K is shown in Fig. 1 for a 600 Hz sine wave input. The measured and calculated sound temperature power spectral densities, shown in Fig. 1(b), reveal agreement within  $\pm 1$  dB for the first three harmonics and a system response 3 dB down point at approximately 2 kHz. This roll-off is consistent with the manufacturer’s data for the upper limit for the frequency response of the wire itself. Note that the asymmetric waveform shape is caused by a combination of nonlinear waveform steepening coupled with boundary layer dispersion in the tube.<sup>12</sup>

## 4. Acoustic temperature measurements in a rocket noise field

### 4.1 Experiment description

Given the relatively high noise floor and limited bandwidth of the temperature probe, a full-scale rocket motor might appear in one sense as an ideal source for acoustic temperature measurements because of the combination of high amplitudes and low frequencies. Consequently,

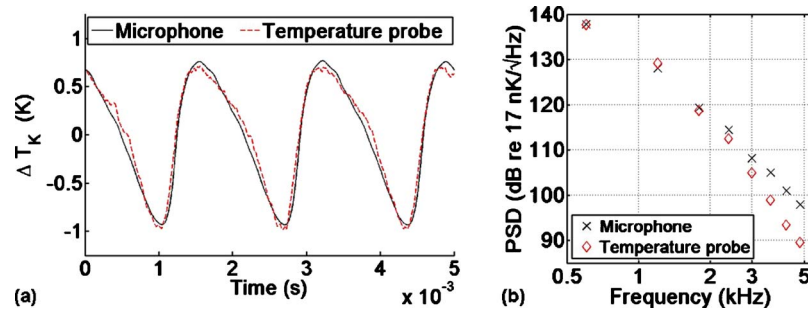


Fig. 1. (Color online) Comparison of measured versus pressure-calculated temperature from a nonlinearly propagated 600 Hz initial sine wave in a plane wave tube. (a) Time waveform comparison. (b) Power spectral density amplitudes of the harmonics present in the acoustic temperature waveforms, which reveals the approximate 2 kHz upper limit of the temperature probe.

the temperature probe was deployed as part of a static rocket motor test on a GEM-60 solid rocket motor at ATK Space Systems in Promontory, UT. The 13.2 m long motor, which is used as a launch booster for the Delta heavy-lift vehicles, has an approximate 90 s burn time during which it produces an average thrust of nearly 890,000 N (200,000 lbf). A photograph from near the end of the motor firing is depicted in Fig. 2(a).

The temperature probe and two GRAS 40DP microphones were located 23 m downstream with an 8 m offset from the shear layer [see Fig. 2(b)]. The distance between the microphones was 3.8 cm with the temperature probe located in between and equidistant from the microphones. Data from one of the microphones were analyzed previously as part of an analysis of the near field noise environment from this motor.<sup>13</sup> At this measurement location, the time-averaged overall sound pressure level was approximately 156 dB re 20  $\mu\text{Pa}$  with the peak spectral levels occurring between 30 and 200 Hz. A ground reflection causes an interference null in the vicinity of 100 Hz, which broadens the peak spectral region beyond what would ordinarily be expected for a power-law-based jet aeroacoustic spectrum.

Although these levels and frequency content are ideal for taking acoustic temperature measurements with the probe, the rocket noise source also represents an extreme environment in which to place a 1  $\mu\text{m}$  diameter wire. Radiant energy from burning aluminum particles in the plume and the likelihood of entrained flow in the near field practically guarantee nonacoustic temperature fluctuations to be present. For the motor test, data collection using the same National Instruments-based data acquisition system was begun with a clock-based trigger at a sampling rate of 204.8 kHz. Meteorological gages with a 1 s sampling interval were used to measure the ambient temperature (also measured with the temperature probe) and the ambient

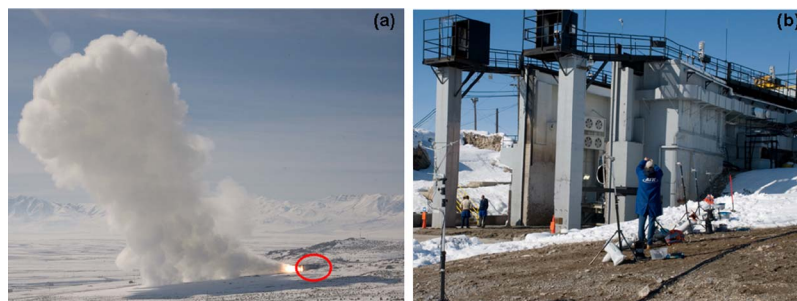


Fig. 2. (Color online) (a) A distant view of the GEM-60 rocket motor near the end of the motor test. (b) The temperature probe and microphones being placed on a tripod near the motor. The building in the background houses the motor (the edge of the nozzle is visible) and is circled in Fig. 2(a) to provide a better sense of scale.

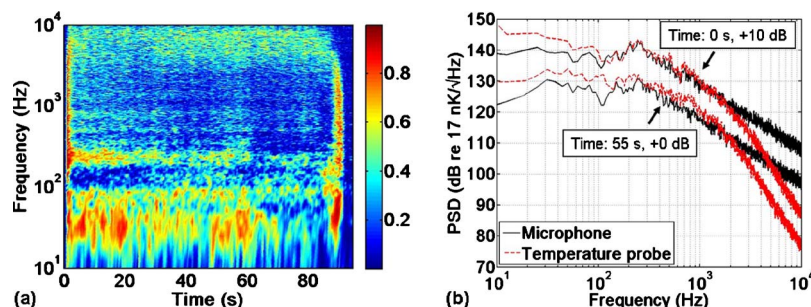


Fig. 3. (Color online) (a) Coherence between the GRAS 40DP 3.8 mm microphone and the temperature probe as a function of time. (b) Sound temperature spectral densities calculated from the temperature probe and GRAS 40DP microphone data during the first 1.28 s of the motor firing (time: 0 s, +10 dB), where a 10 dB offset has been added and later during the firing (time: 55 s, +0 dB).

pressure during the motor firing. During the firing, the average temperature increased by approximately 17 °C and the barometric pressure, as expected, remained essentially constant with insignificant fluctuations.

#### 4.2 Results and analysis

To ensure comparisons can be made between two closely spaced acoustic transducers in this environment, the signals from the two 40DP microphones were first analyzed. Their average spectra, which had the expected power-law shape at low and high frequencies, were virtually identical. Furthermore, and the average coherence between 10 Hz and 2 kHz exceeded 0.98 during the duration of the test. Given the similarity of the acoustic pressure field over the spatial region containing the three sensors, a similar analysis of the coherence between a 40DP microphone and the temperature probe is an important indicator of the relative importance of the acoustic fluctuations during the test. Shown in Fig. 3(a), the coherence was calculated by stepping through the signal in 0.5 s increments and considering a block length of  $2^{18}$  samples, from which 15 averages were calculated using Hanning-windowed subblocks of  $2^{15}$  samples with 50% overlap.

The coherence between the microphone and temperature probe in Fig. 3(a) reveals the presence of significant nonacoustic fluctuations during the firing. At the onset of the test firing, the coherence is relatively high, but drops around the ground-interference null frequency of about 100 Hz. However, as the motor firing progresses, the coherence quickly deteriorates such that the signals have little correlation above a few hundred hertz. At the very end of the test ( $\sim 88$  s), where the motor thrust is rapidly diminishing (see Ref. 13) and the plume environment is contracting, the coherence again improves.

Equation (2) was used to convert the microphone-measured pressure waveform to acoustic temperature, and the sound temperature spectral density from each transducer signal was then estimated. Displayed in Fig. 3(b), the spectra have been calculated over a 1.28 s time window ( $2^{18}$  samples) at the beginning of the test and at 55 s into the firing. The result clearly shows the  $\sim 2$  kHz bandwidth of the temperature probe and the magnitude of the total temperature fluctuations, which are greater than the acoustic fluctuations predicted from the microphone data using Eq. (2).

Examination of the time waveforms is also useful. Displayed in Fig. 4 are two small portions of the time waveforms from the time: 0 s [Fig. 4(a)] and time: 55 s blocks of data [Fig. 4(b)]. Because very low-frequency oscillations measured by the temperature probe but not by the microphone made visual comparison difficult, a zero-phase distortion highpass filter with a 30 Hz cutoff frequency was used to filter both signals. Using the ambient temperature and pressure data, the microphone pressure waveform has been transformed via Eq. (2) to compare directly with the measured temperature data.

In Fig. 4(a), at the beginning of the test, the predicted and measured temperature fluctu-

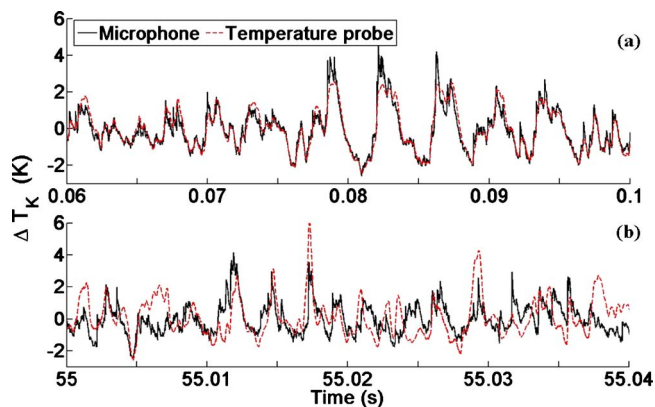


Fig. 4. (Color online) Measured and calculated temperature fluctuations. (a) At the beginning of the motor firing, where agreement between the two transducers is generally good. (b) At 55 s into the firing, where the partial coherence between the signals is evident.

tuations agree very well, with peak fluctuations on the order of 3–4 K. The bandwidth limitation of the temperature probe is evidenced by the increased rise time and reduced amplitude at the shocklike portions of the waveform. The rapid deterioration in coherence, as seen in Fig. 3(a), begins only a few hundred milliseconds into the firing, which explains why the agreement in Fig. 4(a) is better than the average spectral agreement over the first 1.28 s of the firing in Fig. 3(b). In Fig. 4(b), which has the same amplitude scale as Fig. 4(a), the partial coherence between the signals is evident in the way they loosely track each other. The greater amplitude of the temperature oscillations, also present in the spectrum in Fig. 3(b), reveals the significance of the nonacoustic temperature oscillations.

Possible contributors to the nonacoustic temperature oscillations include (a) turbulent entrained flow field near the motor and (b) nonconstant radiative heating effects from the extremely bright but turbulent light source that the plume represents. However, the better agreement between the two sensors near the beginning of the test implies that flow is the primary cause. If radiative heating effects were the dominant cause of the nonacoustic fluctuations, these fluctuations would happen virtually instantaneously after motor ignition. On the other hand, it would take some period of time for a steady-state flow field to begin to be established and the turbulence-related temperature fluctuations to appear. It is also possible that probe heating during the firing could cause increased susceptibility to velocity-related fluctuations, which would increase errors. In any case, the results show the difficulties associated with measuring acoustic fluctuations using this or other fine-wire probes<sup>5</sup> in the presence of turbulent flow.

## 5. Conclusion

In this letter, we have primarily considered the measurement of acoustic temperature fluctuations near a large solid rocket motor. The results have shown that nonacoustic temperature fluctuations significantly contribute, but do not dominate, the total temperature field near the motor. These measurements are significantly more difficult than microphone-based pressure measurements, particularly in the near field of a rocket, where temperature probe survivability is a significant concern. Nevertheless, the fact that a finite-amplitude continuous noise generation by a rocket produces acoustic temperature fluctuations greater than 2 K is a fascinating exercise that can be used to provide insight into the relationships between acoustic field variables.

## Acknowledgments

Derek Thomas provided the initial inspiration and preliminary work on this project. Roy Norris, David Flores, and Kevin Rees of ATK Space Systems Test Services gave invaluable support during the GEM-60 measurements. In addition, Buye Xu is thanked for helpful discussions during the data analysis.

## References and links

- <sup>1</sup>G. R. Ochs, "A resistance thermometer for measurement of rapid air temperature fluctuations," Technical Report No. IER 47-ITSA 46, ESSA, Brussels, Belgium, 1967.
- <sup>2</sup>N. E. J. Boston and E. L. Sipe, "A high frequency platinum resistance thermometer system for measuring turbulent atmospheric temperature fluctuations," Naval Postgraduate School Technical Report, Period 1, July 1974–February 1975 (1975).
- <sup>3</sup>J. C. LaRue, T. Deaton, and C. H. Gibson, "Measurement of high-frequency turbulent temperature," *Rev. Sci. Instrum.* **46**, 757–764 (1975).
- <sup>4</sup>J. Højstrup, K. Rasmussen, and S. E. Larsen, "Dynamic calibration of temperature wires in still air," *DISA Information*, No. 20, 1976, pp. 22–30.
- <sup>5</sup>H.-E. de Bree, "An overview of Microflow Technologies," *Acta. Acust. Acust.* **89**, 1663–172 (2003).
- <sup>6</sup>G. Huelsz and E. Ramos, "Temperature measurements inside the oscillatory boundary layer produced by acoustic waves," *J. Acoust. Soc. Am.* **103**, 1532–1537 (1998).
- <sup>7</sup>G. Huelsz and E. Ramos, "An experimental verification of Rayleigh's interpretation of the Sondhauss tube," *J. Acoust. Soc. Am.* **106**, 1789–1793 (1999).
- <sup>8</sup>G. Braissulis, A. Honkan, J. Andreopoulos, and C. B. Watkins, "Application of hot-wire anemometry in shock-tube flows," *Exp. Fluids* **19**, 29–37 (1995).
- <sup>9</sup>P. M. Morse and K. U. Ingard, *Theoretical Acoustics* (Princeton University Press, New Jersey, 1986), p. 231.
- <sup>10</sup>A. D. Pierce, *Acoustics: An Introduction to Its Physical Principles and Applications* (Acoustical Society of America, New York, 1989), p. 30.
- <sup>11</sup>L. L. Beranek, *Acoustics* (Acoustical Society of America, New York, 1996), p. 39.
- <sup>12</sup>M. F. Hamilton, Y. A. Il'inski, and E. A. Zabolotskaya, "Dispersion," in *Nonlinear Acoustics*, edited by M. F. Hamilton, and D. T. Blackstock (Academic, San Diego, 1998), Chap. 5.
- <sup>13</sup>K. L. Gee, J. H. Giraud, J. D. Blotter, and S. D. Sommerfeldt, "Energy-based acoustical measurements of rocket noise," AIAA Paper No. 2009-3165.